



TITLE:

# Fast thermospheric wind jet at the Earth's dip equator

AUTHOR(S):

Liu, Huixin; Watanabe, Shigeto; Kondo, Tsutomu

---

CITATION:

Liu, Huixin ...[et al]. Fast thermospheric wind jet at the Earth's dip equator. *Geophysical Research Letters* 2009, 36(8): L08103.

ISSUE DATE:

2009-04

URL:

<http://hdl.handle.net/2433/85125>

RIGHT:

Copyright 2009 by the American Geophysical Union.; This is not the published version. Please cite only the published version.; この論文は出版社版ではありません。引用の際には出版社版をご確認ご利用ください。

# 1 **Fast Thermospheric Wind Jet At The Earth's Dip Equator**

Huixin Liu

2 Earth and Planetary Science Division, Hokkaido University, Japan

Shigeto Watanabe

3 Earth and Planetary Science Division, Hokkaido University, Japan

Tsutomu Kondo

4 Earth and Planetary Science Division, Hokkaido University, Japan

---

H. Liu, and S. Watanabe, and Tsutomu Kondo, Earth and Planetary Science Division, Hokkaido University, Sapporo 060-0810, Japan (huixin@ep.sci.hokudai.ac.jp)

X - 2

LIU ET AL.: FAST WIND JET AT THE DIP EQUATOR

5 The thermospheric zonal wind forms a fast wind jet at the Earth's dip  
6 equator instead of the geographic equator. This remarkable feature is re-  
7 vealed in two sets of independent observations made two decades apart. One  
8 is from the CHAMP satellite during the year of 2002 and the other is from  
9 the DE-2 satellite during Aug. 1981 – Feb. 1983. Both observations show  
10 that this wind jet is eastward at night with speed reaching  $150 \text{ ms}^{-1}$ , and  
11 westward around noon with speed over  $75 \text{ ms}^{-1}$ . These fast wind jets are  
12 observed during local times of fully developed equatorial ionization anomaly  
13 (EIA). On the other hand, a channel of slow wind is found on the dip equa-  
14 tor during the period of 05–08 MLT, which corresponds to local times before  
15 the EIA develops. These features strongly suggest the ion drag being the  
16 principle cause for shifting the wind jet from the geographic equator to the  
17 dip equator.

D R A F T

March 10, 2009, 3:39pm

D R A F T

## 1. Introduction

18 The Earth's thermosphere covers the region from about 80 km to 500 km altitude depending  
19 on latitude and local time. Its thermal dynamics are mainly controlled by the solar EUV/UV  
20 heating at low to middle latitudes. From this point of view, the thermosphere forms a high  
21 density bulge at the subsolar point and a density hole at the midnight. This distribution builds  
22 up pressure gradient directing from noon to midnight, which drives thermospheric winds. The  
23 gross structures of the neutral density and wind are described well by empirical models like  
24 MSIS and HWM, with a density maximum at the subsolar point and the strongest wind at the  
25 geographic equator for equinoxes or seasonally averaged case [*Picone et al.*, 2002; *Hedin et al.*,  
26 1996]. However, satellite observations have revealed significant deviations from these gross fea-  
27 tures. In particular, the equatorial ionization anomaly (EIA) [*Namba and Maeda*, 1939; *Apple-*  
28 *ton*, 1946] has been demonstrated to strongly modify the classical picture of the thermosphere.  
29 For instance, the neutral density has been found to form a minimum at the dip equator flanked  
30 by two maxima on both sides [*Hedin and Mayr*, 1973; *Liu et al.*, 2005, 2007], resembling the  
31 latitudinal structure of EIA.

32 The zonal wind has been reported by *Raghavarao et al.* [1991] and *Coley et al.* [1994] to  
33 blow strongest at the Earth's dip equator instead of the geographic equator. Both studies used  
34 the DE-2 measurements during 1981-1983. Due to the lack of neutral wind observations at  
35 upper thermospheric altitudes ( $\sim 400$  km), this important feature has not been corroborated by  
36 independent measurements thereafter. Recently, the CHAMP satellite has been providing in  
37 situ high-resolution thermospheric wind observations in the cross-track direction with a global  
38 coverage [*Liu et al.*, 2006; *Lühr et al.*, 2007; *Förster et al.*, 2008]. A comparison between the

39 CHAMP-derived zonal wind and that predicted by the HWM model in equatorial regions has  
40 revealed satisfactory agreement in most local times [*Liu et al.*, 2006]. Since the HWM model  
41 prediction at the altitude of CHAMP is mainly based on DE-2 measurements, the comparison  
42 was in fact a comparison between the CHAMP and DE-2 measurements. In this paper, we  
43 investigate the latitudinal structure of zonal winds at low and middle latitudes. By comparing  
44 the CHAMP and DE-2 measurements, we aim to examine the global feature of wind jet with  
45 independent observations.

## 2. Data

46 Two sets of independent thermospheric zonal wind measurements are utilized in this study.  
47 One is the 10-s averaged data from the CHAMP satellite and the other is the 16-s averaged data  
48 from the DE-2 satellite. CHAMP is in a near-circular orbit with an inclination of  $87.3^\circ$ . The  
49 average altitude in the year of 2002 is about 410 km. Its orbital plane precesses through all local  
50 times every 3 months. It effectively probes the in-situ wind with an accuracy of  $\sim 20 \text{ ms}^{-1}$ .  
51 The inclination of DE-2 satellite is  $90^\circ$  and has its perigee at around 300 km. The accuracy  
52 of the wind measurements from DE-2 is  $\sim 10 - 20 \text{ ms}^{-1}$ . It samples through all local times  
53 every 6 months. Readers are referred to *Liu et al.* [2006] and *Spencer et al.* [1981] for details  
54 concerning the derivation procedure and related errors about these data.

55 The chosen data periods are Jan. 2002–Dec. 2002 and Aug. 1981–Feb. 1983 for CHAMP  
56 and DE-2, respectively. The year of 2002 is chosen for CHAMP, since the average solar radio  
57 flux value ( $F_{10.7}=179$ ) is comparable to that for DE-2 ( $F_{10.7}=166$ ). Data during very active  
58 periods ( $K_p \geq 5$ ) are excluded in the following analysis.

### 3. Results

59 The seasonally averaged zonal wind distribution in the frame of geographic latitude vs. geo-  
60 graphic longitude is presented in Figure 1 for the period of 18–24 MLT. The upper panel is for  
61 CHAMP and the lower one for DE-2. The solid line depicts the dip equator. We see that the  
62 zonal wind blows eastward at low to middle latitudes as observed by both satellites. The wind  
63 velocity peaks in the equatorial region and decreases towards higher latitudes. An interesting  
64 feature stands out prominently. That is, a banded structure forms along the solid line. In this  
65 band, the maximum wind velocity is found at the Earth’s dip equator, instead of the geographic  
66 equator. The wind speed amounts to nearly  $150 \text{ ms}^{-1}$ , twice as that near  $\pm 25^\circ$  magnetic latitude.  
67 Both the CHAMP and DE-2 observations reveal nearly identical latitudinal pattern.

**Figure 1**

68 We now examine the wind pattern from an alternative perspective. Figure 2 illustrates the zonal  
69 wind distribution in the frame of magnetic dip latitude vs. magnetic local time in quasi-dipole  
70 coordinates. Although some differences exist in the mean values of the wind and also in the  
71 local times of westward-to-eastward wind reversal and the second maximum (which will be  
72 addressed later), both CHAMP and DE-2 observations reveal fairly similar wind patterns. The  
73 wind at equatorial latitudes blows eastward during night and westward before afternoon (14  
74 MLT for CHAMP and 16 MLT for DE-2). Towards higher latitude, the morning wind reversal  
75 from eastward to westward occurs progressively at earlier local times. For instance, the reversal  
76 is at  $\sim 02$  MLT near  $\pm 30^\circ$  latitude in comparison to 05–06 MLT at the dip equator. This leads  
77 to a pronounced triangle shape in the 2-D distribution of the wind shown in Figure 2. On the  
78 nightside, the latitudinal variation of the wind exhibits a maximum at the dip equator (better  
79 seen in the black curves in the right panels of Figure 2). This fast wind jet continues throughout

**Figure 2**

80 the time of eastward wind. During 05–08 MLT, both observations show a minimum westward  
 81 flow at the dip equator sandwiched by faster westward flow at middle latitudes (see pink curves  
 82 in Figure 2). After 09 MLT, however, the strongest westward flow is again found at the dip  
 83 equator (blue curves in Figure 2). In summary, the wind forms a fast eastward jet at the dip  
 84 equator during 18–05 MLT, and a fast westward jet after 09 MLT. During 05–08 MLT, the dip  
 85 equator becomes a channel of slow wind. There is good agreement on these trends revealed by  
 86 CHAMP and DE-2 observations.

#### 4. Discussion

87 The above analysis of the latitudinal structure of the thermospheric zonal wind has revealed a  
 88 fast wind jet at the Earth’s dip equator in both the CHAMP and DE-2 observations (see Figure  
 89 1). It is remarkable to see how similar this structure is in two independent datasets obtained two  
 90 decades apart with totally different instruments. The CHAMP probes the in-situ neutral wind  
 91 with a tri-axis accelerometer, while the DE-2 measured the wind with a wind and temperature  
 92 spectrometer. The principles of these instruments are completely different as described in *Liu*  
 93 *et al.* [2006] and *Spencer et al.* [1981]. Furthermore, the neutral wind varies significantly with  
 94 location, season, solar and geomagnetic conditions [*Liu et al.*, 2004, 2006]. Given these intrinsic  
 95 variability and the totally different observing techniques, the consistency between latitudinal  
 96 structures revealed in the two datasets is striking. The CHAMP observations corroborate the  
 97 DE-2 measurements, and strongly confirm the existence of the fast wind jet and its stable  
 98 location at the dip equator.

99 This wind jet along the Earth’s dip equator instead of the geographic equator demonstrates  
 100 strong magnetic control of the thermospheric dynamic. In the upper atmosphere at low latitudes,

101 the atmospheric pressure gradient is the primary driver of the neutral wind, with the ion drag  
 102 being an important impeding force. It regulates the neutral wind considerably [*Rishbeth, 1972*].  
 103 With the development of the EIA structure in the equatorial ionosphere after  $\sim 09$  MLT, the  
 104 plasma density forms a trough at the dip equator [*Balan and Bailey, 1995*]. This consequently  
 105 leads to lower ion drag, which facilitates faster wind to flow at the dip equator. During the  
 106 period of 05–08 MLT, however, the EIA structure disappears and a peak of the plasma density  
 107 forms at the dip equator instead of a trough [*Lin et al., 2007*]. This causes the ion drag to peak  
 108 at the dip equator as well, hence to slow down the zonal wind considerably. As a result, the  
 109 dip equator becomes a channel of slow flow instead of fast flow. The local time variation of  
 110 the wind jet examined in section 3 shows this is exactly the case. Fast wind jet is found at the  
 111 dip equator during 18–05 MLT and after 09 MLT, while slow wind presents during 05–08 MLT.  
 112 These observations strongly suggest the ion drag being the principle cause for shifting the fast  
 113 wind jet from the geographic equator to the dip equator.

114 Besides the similar latitudinal structure revealed by CHAMP and DE-2, we note that an ap-  
 115 parent difference is seen in the occurring time of westward-to-eastward wind reversal and the  
 116 second wind maximum after midnight. The reversal is around 13–14 MLT for CHAMP, while  
 117 around 16–17 MLT for DE-2. The second wind maximum is around 01 MLT for CHAMP, while  
 118 near 03 MLT for DE-2 (see Figure 2). Along with differences in the mean values of the wind  
 119 speed, they likely arise from several sources as previously pointed out in [*Liu et al., 2006*]. First,  
 120 seasonal average. Due to the slow precessing rate of DE-2's orbital plane, the DE-2 dataset suf-  
 121 fers strongly from the locking between local time and season. The midnight/noon sectors were  
 122 predominantly sampled around equinoxes, while the dawn/dusk sectors around solstices. Since



123 CHAMP transverses all local times every 3 months, each local time is equally sampled in four  
 124 seasons in one year. Second, altitude average. The altitude of DE-2 measurements ranges from  
 125 200–700 km, while CHAMP measurements are collected within a much smaller altitude range  
 126 between 400–430 km. Third, some discrepancies arising from different instruments used by  
 127 DE-2 and CHAMP cannot be ruled out. These differences between the two sets of measure-  
 128 ments may have contributed to the above-mentioned discrepancies.

129 Finally, it is worth pointing out that except for at  $\sim 20$  MLT, no bands of slow wind near  $\pm 25^\circ$   
 130 latitude is discernible (see e.g., Figure 1). This is different from that reported in *Raghavarao*  
 131 *et al.* [1991]. In their study, *Raghavarao et al.* examined the latitudinal variation of the wind or-  
 132 bit by orbit instead of in a statistical manner as we do here. As shown in Figure 1 of *Raghavarao*  
 133 *et al.* [1991], for instance, the wind peak at the dip equator is very prominent and broad, with  
 134 a width about  $20^\circ$  in latitude. But the wind trough near  $\pm 25^\circ$  latitude is much narrower ( $\sim 7^\circ$ ).  
 135 Furthermore, the location of the wind trough is expected to be highly variable with season, fol-  
 136 lowing that of the EIA crests. Therefore, it is quite likely that this narrow trough structure with  
 137 shallow magnitude has been smeared out in statistical analysis, as a consequence of combing  
 138 measurements in different season, longitudes and local times. The statistical analysis of the  
 139 DE-2 wind in *Coley et al.* [1994] has revealed no band of slow wind either, consistent with our  
 140 results. The exception around 20 MLT (see right panels of Figure 2), with a subtle signature  
 141 of slow winds near  $\pm 20^\circ$  magnetic latitude, is likely due to the post-sunset enhancement of the  
 142 EIA [*Balan and Bailey*, 1995]. This enhanced EIA leads to a much more significant depres-  
 143 sion of the zonal wind in crest regions than at other local times, which could have survived the  
 144 statistical averages.

145 In summary, both the CHAMP and DE-2 observations reveal a fast wind jet at the Earth's  
146 dip equator instead of the geographic equator, demonstrating the strong magnetic control of the  
147 neutral dynamics via ion drag.

148 **Acknowledgments.** We thank W. Köhler for processing the CHAMP data. The work of HL is  
149 supported by the JSPS foundation. The CHAMP mission is supported by the German Aerospace  
150 Center (DRL) in operation and by the Federal Ministry of Education and Research (BMBF) in  
151 data processing.

## References

- 152 Appleton, E. V. (1946), Two anomalies in the ionosphere, *Nature*, *157*, 691.
- 153 Balan, N., and G. J. Bailey (1995), Equatorial plasma fountain and its effects: Possibility of an  
154 additional layer, *J. Geophys. Res.*, *100*, 21,421–21,432, doi:10.1029/95JA01555.
- 155 Coley, W. R., R. A. Heelis, and N. W. Spencer (1994), Comparison of low-latitude ion and  
156 neutral zonal drift using DE2 data, *J. Geophys. Res.*, *99*, 341–348.
- 157 Förster, C., S. Rentz, W. Köhler, H. Liu, and S. E. Haaland (2008), IMF dependence of high-  
158 latitude thermospheric wind pattern derived from CHAMP cross-track measurements, *Ann.*  
159 *Geophys.*, *26*, 1581–1595.
- 160 Hedin, A. E., and H. G. Mayr (1973), Magnetic control of the near equatorial neutral thermo-  
161 sphere, *J. Geophys. Res.*, *78*, 1688–1691.
- 162 Hedin, A. E., et al. (1996), Empirical wind model for the upper, middle and lower atmosphere,  
163 *J. Atmos. Solar-Terr. Phys.*, *58*, 1421–1447.

- 164 Lin, C. H., J. Y. Liu, T. W. Fang, P. Y. Chang, H. F. Tsai, C. H. Chen, and C. C. Hsiao (2007),  
165 Motions of the equatorial ionization anomaly crests imaged by FORMOSAT-3/COSMIC,  
166 *Geophys. Res. Lett.*, *34*, L19101, doi:10.1029/2007GL030741.
- 167 Liu, H., H. Lühr, V. Henize, and W. Köhler (2005), Global distribution of the thermo-  
168 spheric total mass density derived from CHAMP, *J. Geophys. Res.*, *110*, A04301, doi:  
169 10.1029/2004JA010741.
- 170 Liu, H., H. Lühr, S. Watanabe, W. Köhler, V. Henize, and P. Visser (2006), Zonal winds in  
171 the equatorial upper thermosphere: decomposing the solar flux, geomagnetic activity, and  
172 seasonal dependencies, *J. Geophys. Res.*, *111*, A09S29, doi:10.1029/2005JA011415.
- 173 Liu, H., H. Lühr, and S. Watanabe (2007), Climatology of the Equatorial Mass Density  
174 Anomaly, *J. Geophys. Res.*, *112*, A05305, doi:10.1029/2006JA012199.
- 175 Liu, L., X. Luan, W. Wan, J. Lei, and B. Ning (2004), Solar activity variations of  
176 equivalent winds derived from global ionosonde data, *J. Geophys. Res.*, A12305, doi:  
177 10.1029/2004JA010574.
- 178 Lühr, H., S. Rentz, P. Ritter, H. Liu, and K. Häusler (2007), Average thermospheric wind pat-  
179 terns over the polar regions, as observed by CHAMP, *Ann. Geophys.*, *25*, 1093–1101.
- 180 Namba, S., and K.-I. Maeda (1939), *Radio wave propagation*, 86 pp., Corona Publishing,  
181 Tokyo.
- 182 Picone, J. M., A. E. Hedin, D. P. Drob, and A. C. Aikin (2002), NRLMSISE-00 empirical model  
183 of the atmosphere: Statistical comparisons and scientific issues, *J. Geophys. Res.*, *107*, 1468,  
184 doi:10.1029/2002JA009430.

- 185 Raghavarao, R., L. E. Wharton, N. W. Spencer, H. G. Mayr, and L. H. Brace (1991), An equa-  
186 torial temperature and wind anomaly (ETWA), *Geophys. Res. Lett.*, *18*(7), 1193–1196.
- 187 Rishbeth, H. (1972), Thermospheric winds and the F-region: A review, *J. Atmos. Terr. Phys.*,  
188 *34*, 1–47.
- 189 Spencer, N. W., L. E. Wharton, H. B. Niemann, A. E. Hedin, G. R. Carignan, and J. C. Maurer  
190 (1981), The Dynamics Explorer wind and temperature spectrometer, *Space Sci. Instrum.*, *5*,  
191 417–428.

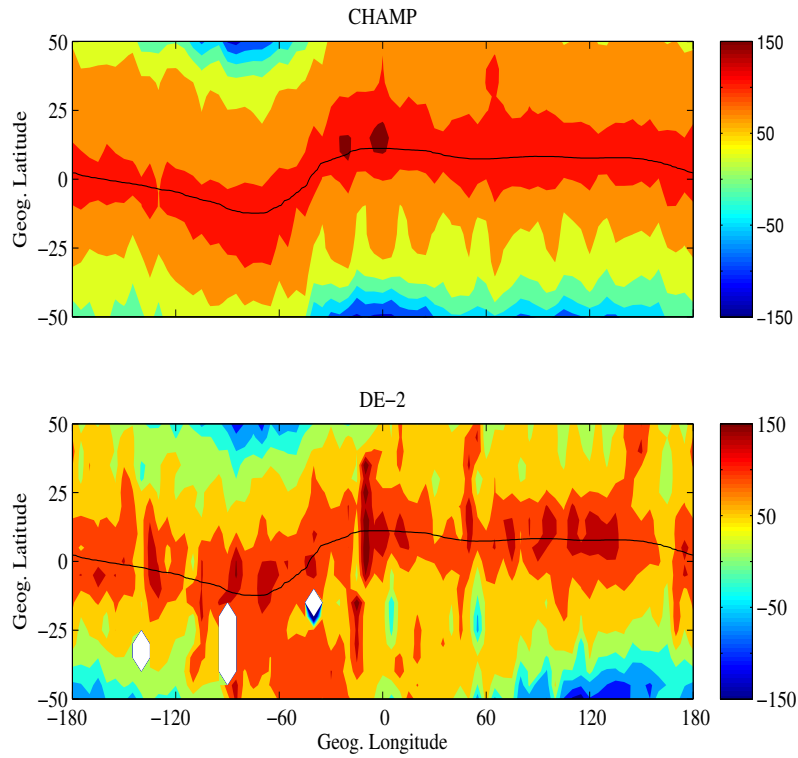


**Figure 1.** Distribution of the seasonally averaged zonal wind velocity (in unit of  $\text{ms}^{-1}$ ) in the frame of geographic longitude vs. geographic latitude during periods of 18–24 MLT. Positive means eastward. The upper panel is for CHAMP and the lower panel for DE-2. The solid line indicates the dip equator. Note the banded structure along the dip equator, where the fastest wind flows.

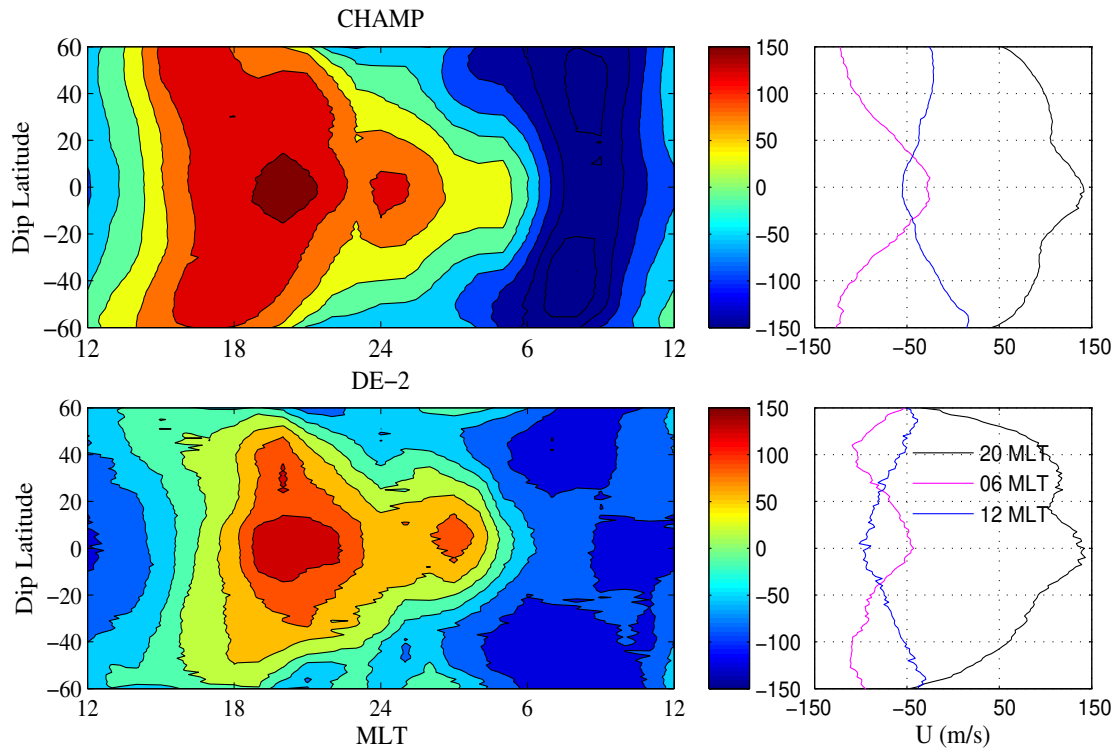


**Figure 2.** Distribution of the seasonally averaged zonal wind velocity (in unit of  $\text{m s}^{-1}$ ) in the frame of magnetic dip latitude vs. magnetic local time in quasi-dipole coordinates. Positive means eastward. The upper row is for CHAMP and the lower row for DE-2. Corresponding latitudinal profiles at 06 MLT, 12 MLT, and 20 MLT are shown in the right panels.